

- BERKOVITCH-YELLIN, Z., ARIEL, S. & LEISEROWITZ, L. (1983). *J. Am. Chem. Soc.* **105**, 765-767.
- BERKOVITCH-YELLIN, Z. & LEISEROWITZ, L. (1977). *J. Am. Chem. Soc.* **99**, 6106-6107.
- BERKOVITCH-YELLIN, Z. & LEISEROWITZ, L. (1980). *J. Am. Chem. Soc.* **102**, 7677-7690.
- BERKOVITCH-YELLIN, Z. & LEISEROWITZ, L. (1982). *J. Am. Chem. Soc.* **104**, 4052-4064.
- BERKOVITCH-YELLIN, Z., VAN MIL, J., ADDADI, L., IDELSON, M., LAHAV, M. & LEISEROWITZ, L. (1985). *J. Am. Chem. Soc.* In the press.
- BOLHUIS, F. VAN (1971). *J. Appl. Cryst.* **4**, 263-264.
- EISENSTEIN, M. (1981). PhD Thesis, Feinberg Graduate School, Weizmann Institute of Science, Rehovot, Israel.
- HIRSHFELD, F. L. (1976). *Acta Cryst.* **A32**, 239-244.
- HIRSHFELD, F. L. (1977). *Isr. J. Chem.* **16**, 226-229.
- HUANG, C.-M., LEISEROWITZ, L. & SCHMIDT, G. M. J. (1973). *J. Chem. Soc. Perkin Trans. 2*, pp. 503-508.
- KARTHA, G. & DE VRIES, A. (1961). *Nature (London)*, **192**, 892.
- LEISEROWITZ, L. (1976). *Acta Cryst.* **B32**, 775-802.
- SHELDRIK, G. M. (1976). *SHELX*. Program for crystal structure determination. Univ. of Cambridge, England.
- VERBIST, J. J., LEHMANN, M. S., KOETZLE, T. F. & HAMILTON, W. C. (1972). *Acta Cryst.* **B28**, 3006-3013.
- WANG, J. L. W. (1983). MSc Thesis, Feinberg Graduate School, Weizmann Institute of Science, Rehovot, Israel.
- WEINSTEIN, S. (1982). *Angew. Chem. Int. Ed. Engl.* **21**, 218.

Acta Cryst. (1985). **B41**, 348-354

Trimesic Acid, Its Hydrates, Complexes and Polymorphism. VIII.* Interstitial Complexes of α - and (the Hypothetical) γ -Trimesic Acid

BY F. H. HERBSTEIN, M. KAPON AND G. M. REISNER

Department of Chemistry, Technion-Israel Institute of Technology, Haifa, Israel 32000

(Received 12 April 1984; accepted 23 April 1985)

Abstract

Interstitial complexes of α -trimesic acid [TMA; Duchamp & Marsh (1969). *Acta Cryst.* **B25**, 5-19] have been prepared with guests such as Br₂ and acetone (composition TMA. $\frac{1}{6}$ X), and with hydroquinone and resorcinol (composition TMA. $\frac{1}{12}$ X). These complexes are isomorphous with α -TMA; e.g. TMA. $\frac{1}{6}$ Br₂ is monoclinic, *C2/c* with $a = 26.510$ (2), $b = 16.449$ (5), $c = 26.580$ (7) Å, $\beta = 91.80$ (1)°, $Z = 48$. The structure was refined to $R = 11.1\%$. Determination of the structure showed that the Br₂ molecules are accommodated in a considerably disordered manner in cavities around $0, \frac{1}{2}, \frac{1}{4}$. High-temperature studies show that α -trimesic acid transforms enantiotropically to a polycrystalline β -phase at ~ 543 K which melts at ~ 603 K. Single crystals of a third phase, γ , are formed by condensation of the vapour on cold surfaces. The γ -phase is isostructural [orthorhombic, *I222*, $a = 24.225$ (7), $b = 15.364$ (5), $c = 16.562$ (6) Å, $Z = 24$] with TMA.I₅ [Herbstein, Kapon & Reisner (1981). *Proc. R. Soc. (London) Ser. A*, **376**, 301-318]. The structure was refined to $R = 8.4\%$. The channel along $0, 0, z$ which contains the linear I₅ anions in TMA.I₅ was found to be empty in γ -TMA. The cavity around $\frac{1}{2}, 0, \frac{1}{2}$, which contains disordered water molecules in TMA.I₅, here accommodates disordered TMA and various benzenedicarboxylic acids, which are presumed to stabilize the γ -phase.

* Part VII: Herbstein, Kapon & Reisner (1981).

Introduction

The crystal structure of α -trimesic acid (TMA; 1,3,5-benzenetricarboxylic acid) is characterized by the mutual triple catenation of pleated hexagonal networks of hydrogen-bonded TMA molecules (Duchamp & Marsh, 1969). Analogous mutual triple catenation of TMA networks has been found in TMA.0.7H₂O.0.09HI₅(TMA.I₅) where the networks are planar and so arranged as to leave channels in which the pentaiodide ions are constrained from their usual V-shape to a linear configuration (Herbstein, Kapon & Reisner, 1981). The α -TMA structure is tightly packed but nevertheless complexes of composition TMA. $\frac{1}{6}$ Br₂ and TMA. $\frac{1}{12}$ I₂ have been reported (Herbstein, 1968), with the halogen molecules presumably located in interstitial sites. Furthermore, we have found (unpublished results) that α -TMA appears to undergo phase transitions at high temperatures [the melting point of TMA is given as ~ 653 K (*Dictionary of Organic Compounds*, 1965)]. Interrelationships between these facets of the structural chemistry of trimesic acid are presented here.

Interstitial complexes of α -TMA

Experimental

Trimesic acid was crystallized from saturated aqueous solutions of the five guest molecules studied here (for picric acid as a guest see Appendix 1). Deep-red and deep-purple crystals, respectively, of

Table 1. Crystal data; cell dimensions measured on a four-circle diffractometer with Mo $K\alpha$ [except for α -TMA, see note (1)]

Compound	α -TMA ⁽¹⁾	α -TMA. $\frac{1}{8}\text{Br}_2$	α -TMA. $\frac{1}{8}$ acetone	α -TMA. $\frac{1}{2}\text{I}_2$	α -TMA. $\frac{1}{12}$ resorcinol	α -TMA. $\frac{1}{12}$ hydroquinone	TMA.0.7H ₂ O. 0.09H ⁽²⁾	γ -TMA ⁽³⁾
Space group	<i>C</i> 2/ <i>c</i>	<i>C</i> 2/ <i>c</i>	<i>C</i> 2/ <i>c</i>	<i>C</i> 2/ <i>c</i>	<i>C</i> 2/ <i>c</i>	<i>C</i> 2/ <i>c</i>	<i>I</i> 222	<i>I</i> 222
<i>a</i> (Å)	26.520 (2)	26.510 (7)	26.541 (7)	26.541 (7)	26.557 (7)	26.531 (7)	21.945 (7)	24.225 (7)
<i>b</i> (Å)	16.420 (1)	16.449 (5)	16.482 (5)	16.457 (5)	16.434 (5)	16.450 (5)	17.917 (6)	15.364 (5)
<i>c</i> (Å)	26.551 (2)	26.580 (7)	26.604 (7)	26.530 (7)	26.585 (7)	26.559 (7)	16.711 (6)	16.562 (6)
β (°)	91.53 (1)	91.80 (1)	92.65 (1)	91.58 (1)	91.97 (5)	92.01 (5)	—	—
<i>V</i> (Å ³)	115.58	115.85	116.25	115.83	115.96	115.84	6571	6164
<i>Z</i>	48	48	48	48	48	48	24	24
<i>M_r</i>	210.1	236.8	219.8	231.3	219.3	219.3	279.7	227.7
<i>D_x</i> (g cm ⁻³)	1.45	1.63	1.51	1.59	1.51	1.51	1.71	1.47
<i>D_x</i> ⁽⁴⁾ (g cm ⁻³)	1.46	1.62	1.50	1.59	1.52	1.52	1.70	1.47

Notes: (1) Duchamp & Marsh (1969), back-reflection Weissenberg method, Cu $K\alpha_{1,2}$. (2) Herbstein, Kapon & Reisner (1981). (3) TMA.0.05TMA.0.04C₆H₄(COOH)₂. (4) Densities were measured by flotation in *sym*-tetrabromoethane-toluene mixtures.

the same habit as α -TMA, were obtained with Br₂ and I₂ as guests. The other guests gave colourless crystals visually indistinguishable from those of α -TMA. Crystal data are given in Table 1. Presence of the guests was established by the colour changes (when applicable), density measurements, chemical analyses (results deposited)* and mass spectroscopic and NMR analyses. Additional proof, apart from density measurements and chemical analyses, was considered to be important in establishing the presence of hydroquinone, resorcinol and acetone. Thus, mass spectra were determined for all three complexes as a function of sample temperature (Atlas Mat model CH4 under electron impact energy of 70 eV). The room-temperature spectra showed trimesic acid only. The spectra of the guest molecules appeared when the complexes were heated to 523–543 K. For TMA. $\frac{1}{12}$ (hydroquinone) an ¹H NMR spectrum was also taken (Varian XL-200FT, sample dissolved in DMSO, room temperature). It consists of two strong sharp signals at 8.56 and 6.52 p.p.m. (relative to TMS), which are ascribed to the aromatic hydrogens of TMA and hydroquinone, respectively. The relative intensities of the TMA and hydroquinone signals are close to the expected ratio of 9:1.

Crystal structure of α -TMA. $\frac{1}{8}\text{Br}_2$

Experimental

Widespread occurrence of twinning about (101) and/or (10 $\bar{1}$) in α -TMA was reported by Duchamp & Marsh (1969); we find frequent twins among the

* Results of chemical analyses for the interstitial complexes of α -TMA, lists of structure factors for α - and γ -TMA, final positional parameters and anisotropic temperature factors of the TMA molecules of α -TMA, final positional parameters, occupancies and isotropic temperature factors of the disordered moieties around $\frac{1}{2}$, 0, $\frac{1}{2}$ in γ -TMA, anisotropic temperature factors of the TMA molecules of γ -TMA, and Appendix 2 have been deposited with the British Library Lending Division as Supplementary Publication No. SUP 42191 (52 pp.). Copies may be obtained through The Executive Secretary, International Union of Crystallography, 5 Abbey Square, Chester CH1 2HU, England.

interstitial complexes. The twins are presumably polysynthetic as they are not detectable under a polarizing microscope. Precession photographs (Cu $K\alpha$) of a crystal mounted about [010] showed that reciprocal layers normal to a purported *c* axis were actually composites of an *h*, *k*, *l* layer from individual 1 and *h*, *k*, *l* layer from individual 2 (*l*₁ = *h*₂), and conversely for a purported *a* axis. Because *d*₁₀₀ and *d*₀₀₁ differ by only 0.1% these superimposed sections of the reciprocal lattice appear as single layers. This is the basis for the Duchamp & Marsh method of detecting twinning by observing the appearance of reflections in apparent violation of the extinction condition for *C*-centring. On an (*hkl*)₁ layer the deviants will be (*hkl*)₂ reflections (*l*₁ = *h*₂). The twinning is by reticular pseudomerohedry (Cahn, 1954) and the obliquities for twinning on (101) and (10 $\bar{1}$) are 0.06 and 0.16°, respectively. An untwinned crystal was found after some effort. Cell dimensions are in Table 1 and experimental details in Table 2. Using the positional parameters of the isomorphous α -TMA, the structure was refined to *R* = 24% [refinement on *F* using *SHELX77* (Sheldrick, 1977)]. A difference Fourier synthesis calculated at this stage showed strong residual electron densities around the twofold axis at *y* = 0.5, the highest values being about 5 e Å⁻³. The chemical analysis and measured density show that there are eight Br₂ molecules in the unit cell; thus each of the four cavities in the unit cell must contain two Br₂ molecules related by a twofold axis. However, considerable disorder was found among the possible Br positions and we proceeded as follows. The difference synthesis showed 14 peaks with electron density greater than 1 e Å⁻³ and only these were taken into account in the least-squares refinement. Anisotropic refinement of the TMA molecules and of the 'major orientation' of the Br₂ molecule [Br(1)–Br(2)] together with isotropic refinement of the other Br positions led to convergence at *R* = 11%. Calculated positions of the H atoms (of the benzene rings only) were introduced and refined with fixed temperature factors. Block-matrix refinement was used throughout the final least-squares cycles because of the large

Table 2. *Experimental conditions and refinement data (Philips PW 1100/20 four-circle diffractometer, graphite-monochromated Mo K α , absorption corrections not applied)*

	γ -TMA	α -TMA $\cdot\frac{1}{6}$ Br $_2$
Crystal shape and size	Thin laths (0.1 \times 0.3 \times 0.5 mm)	Red cubes (edge 0.3 mm)
Absorption coefficient	0.83 cm $^{-1}$	14.40 cm $^{-1}$
Measurement mode	$\omega/2\theta$	$\omega/2\theta$
θ limits	2.5 $^\circ$ \leq θ \leq 23.0 $^\circ$	2.5 \leq θ \leq 20 $^\circ$
Scan speed	1.0 $^\circ$ (ω) min $^{-1}$	1.5 $^\circ$ (ω) min $^{-1}$
Scan width	1.20 $^\circ$ (ω)	1.5 $^\circ$ (ω)
Standard reflections	431, 431, 440 (no variation)	113, 661, 661 (no variation)
No. of independent reflections measured	2479	8059
Limits on indices	0 \leq h \leq 26 0 \leq k \leq 16 0 \leq l \leq 18	-28 \leq h \leq 28 0 \leq k \leq 18 0 \leq l \leq 28
Restrictions on reflections	$F_o \geq 1.5\sigma(F_o)$	$F_o \geq 1.5\sigma(F_o)$
No. of reflections in final refinement cycle	1925	4897
No. of parameters refined	1st block 274 2nd block 164	1st block 290 2nd block 290 3rd block 356
R_{int}	0.02 (by merging 220 hkl and $h\bar{k}l$ equivalent reflections)	0.033 (by merging $h\bar{k}l$ and $h\bar{k}0$ equivalent reflections)
R_F	0.084	0.111
Weighting scheme	Unit weights	Unit weights

number of parameters (931). Terminal Δ/σ 's are about 0.5 and a final difference synthesis showed $\Delta\rho$ excursions in the range -0.5 to $+0.8$ e \AA^{-3} , with residual electron densities concentrated in the region of the Br $_2$ molecules. Final positional parameters, occupancies and temperature factors of the disordered Br atoms are listed in Table 3; part of the structure is shown in Fig. 1.

Results and discussion

Pairs of molecules of type *A* (using the nomenclature employed for α -TMA by Duchamp & Marsh) are hydrogen bonded to one another across the twofold axis as well as to molecules of type *C* so as to form an almost planar six-molecule hexagon approxi-

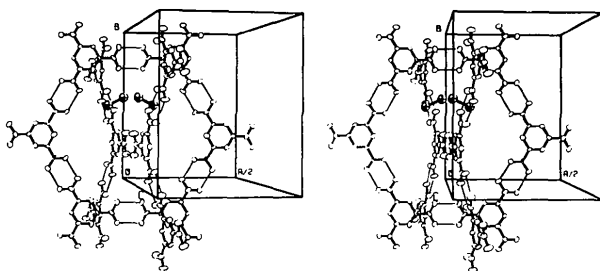


Fig. 1. α -TMA $\cdot\frac{1}{6}$ Br $_2$: ORTEP (Johnson, 1965) stereodiagram showing part of the structure around the twofold axis along 0, $y, \frac{1}{2}$. Only the central member of each of the two triple networks of hydrogen-bonded TMA molecules is shown, and only one of the Br $_2$ orientations [Br(1)-Br(2)]. The larger cavity referred to in the text is occupied by the Br $_2$ molecules while the smaller one is empty.

Table 3. *Final fractional coordinates ($\times 10^3$), occupancies and temperature factors ($\text{\AA}^2 \times 10^3$) of the Br atoms in α -TMA $\cdot\frac{1}{6}$ Br $_2$*

Br(1) and Br(2) were refined anisotropically. $U_{eq} = \frac{1}{3} \sum_i \sum_j U_{ij} a_i^* a_j^* (\mathbf{a}_i \cdot \mathbf{a}_j)$; $\sigma(U_{eq})$ was calculated according to Schomaker & Marsh (1983).

	x	y	z	Occupancy †	U_{eq}/U_{iso}
Br(1)	-19 (1)	545 (1)	162 (1)	0.20	105 (13)
Br(2)	-89 (1)	496 (1)	226 (1)	0.20	133 (11)
Br(3)	-84 (1)	518 (1)	176 (1)	0.15	130 (6)
Br(4)	11 (1)	541 (2)	175 (1)	0.10	149 (11)
Br(5)	-96 (2)	480 (3)	199 (2)	0.15	102 (7)
Br(6)	-119 (1)	503 (2)	133 (1)	0.15	112 (6)
Br(7)	-61 (1)	521 (2)	216 (1)	0.10	149 (8)
Br(8)	-100 (1)	514 (1)	153 (1)	0.15	103 (5)
Br(9)	-80 (1)	565 (1)	146 (1)	0.15	107 (5)
Br(10)	-79 (1)	510 (1)	254 (1)	0.10	133 (9)
Br(11)	-59 (1)	543 (1)	172 (1)	0.10	96 (6)
Br(12)	-112 (1)	462 (1)	165 (1)	0.15	102 (5)
Br(13)	-27 (2)	533 (2)	193 (1)	0.10	121 (8)
Br(14)	54 (1)	517 (2)	216 (2)	0.10	133 (14)

† The occupancies are such that 7.6 (out of 8) Br $_2$ molecules are accounted for.

mately perpendicular to *c*. Similarly, molecules *B* are bonded to one another across the twofold axis and to molecules of type *D* to form a hexagon approximately perpendicular to *a*. These interpenetrate so as to leave two cavities centred along the twofold axis, a larger cavity around $y=0.5$ and a smaller one at $y=0$, the different size of the cavities being due to the unsymmetrical mutual interpenetration. Molecules *E* and *F* are not shown in Fig. 1. Our final TMA coordinates are remarkably close to those of α -TMA (although less accurate). However, there are consistent small differences which appear mainly in the *y* coordinates. The *x* and *z* coordinates of the TMA molecules in α -TMA and α -TMA $\cdot\frac{1}{6}$ Br $_2$ are almost identical (within their e.s.d.'s), but there are differences of more than 10σ (~ 0.1 \AA) between the respective *y* coordinates. These differences are less pronounced for molecules *E* and *F* which are remote from the twofold axis. The differences in the *y* coordinates are such that the entire hexagon perpendicular to *c* moves up along *b* whereas that perpendicular to *a* moves in the opposite direction, the net result being an increase in the size of the cavity at $y=0.5$ and a corresponding decrease of that at $y=0$. Thus, the existence of two cavities along the twofold axis gives the TMA networks a certain flexibility in the *y* direction, without changing the length of *b*. The cavity around $y=0.5$ contains the Br $_2$ molecules whereas no residual electron density was found in the cavity around $y=0$. The value of d (Br-Br) would be expected to be close to that of the free molecule in the gas phase, *i.e.* 2.284 \AA (Karle, 1955); nineteen distances in the range 2.1-2.7 \AA were found between the fourteen atoms of Table 3. Clearly, we have not resolved the disorder of the Br $_2$ molecules; the Br $_2$ molecule in Fig. 1 is based on Br(1) and Br(2) ($d=2.65$ \AA) of Table 3 and is intended as illustrative only.

Solid-state transformations in trimesic acid heated above 523 K

Experimental

The methods used include DTA, high-temperature microscopy and high-temperature X-ray diffraction. Single crystals of α -TMA examined on a hot stage become opaque at ~ 603 K and the liquid evaporates in a flash at ~ 613 K, condensing as long thin laths on nearby cooler surfaces. DTA (Fig. 2) and high-temperature powder diffraction experiments (Fig. 3; cf. Weissman, 1973; Herbstein & Kaftory, 1981; Herbstein, Kapon & Weissman, 1982) showed that the transformations can be summarized as in Table 4. The β -phase has only been obtained in polycrystalline form and we have not been able to retain it on cooling to room temperature. The γ -phase can be cooled to room temperature without change and its crystal structure is reported below. It is stable at 298 K when sealed in a capillary but transforms to an unidentified phase if exposed to the atmosphere. Heating the γ -phase at ~ 1 K min^{-1} gives the β -phase. The vapour pressure of TMA has been measured over the temperature range 553–593 K, which overlaps closely with the region of stability of the β -phase (Kraus, Beránek, Kochloeff & Bažant, 1962). Thus these P - T curves will not be expected to show evidence for solid-state transformations.

Crystal structure of the γ -phase

Experimental

Long thin laths of the γ -phase are formed from the vapour obtained by heating α -TMA to ~ 613 K; the crystals condense on cooler surfaces. Preliminary Weissenberg photography was used to check crystal quality and absence of twinning. A suitable crystal was found after some effort and cell dimensions were measured on the four-circle diffractometer (Table 1). The density calculated for 24 TMA molecules in the unit cell is 1.359 g cm^{-3} , about 8% less than the measured value of 1.47 g cm^{-3} . Proton NMR spectra (Bruker WP-200SY) of γ -phase crystals dissolved in deuterated DMSO showed that benzenedicarboxylic acids were present in addition to TMA, the total impurity content being about 4% of the TMA. A calculated density of 1.47 g cm^{-3} , in good agreement

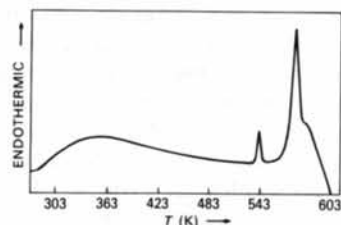


Fig. 2. DTA curve obtained by heating α -TMA (heating rate 10K min^{-1}).

Table 4. Summary of solid-state transformations occurring in α -trimesic acid heated above 523 K (the temperatures are accurate to within ± 5 K; the onset of events is sometimes difficult to establish)

(1) α -TMA as starting material

Sequence (i)

Heating: α -TMA $\xrightarrow{543\text{ K}}$ β -phase $\xrightarrow{603\text{ K}}$ melt $\xrightarrow{\sim 613\text{ K}}$ vapour
Cooling: vapour \rightarrow γ -phase

Sequence (ii)

Heating: α -TMA $\xrightarrow{543\text{ K}}$ β -phase
Cooling: β -phase $\xrightarrow{553\text{ K}}$ γ -phase

Sequence (iii)

Cooling: melt \rightarrow γ -phase

(2) γ -Phase as starting material

Heating: γ -phase $\xrightarrow{\sim 543\text{ K}}$ β -phase \rightarrow melt \rightarrow vapour
Cooling: vapour \rightarrow γ -phase

Notes: The α -phase is monoclinic α -TMA; crystal structure by Duchamp & Marsh (1969). The β -phase is a high-temperature phase of unknown structure and composition. The γ -phase is orthorhombic; the crystal structure reported in the present paper shows that it is $\sim 96\%$ TMA and 4% various benzenedicarboxylic acids.

with the observed value, is obtained on the basis of 24 formula units of composition $\text{TMA}_0.05\text{TMA}_0.04\text{C}_6\text{H}_4(\text{COOH})_2$ in the unit cell. We note that Shishmina, Belikhmaer, Sarymsakov, Koroleva, Sartova & Zhumanalieva (1982) have reported that TMA loses CO_2 on heating above ~ 553 K.

Comparison of cell dimensions (Table 1) shows that γ -TMA and TMA.I_5 are closely related. The resemblance is close enough to permit use of the coordinates of the TMA framework in TMA.I_5 as a

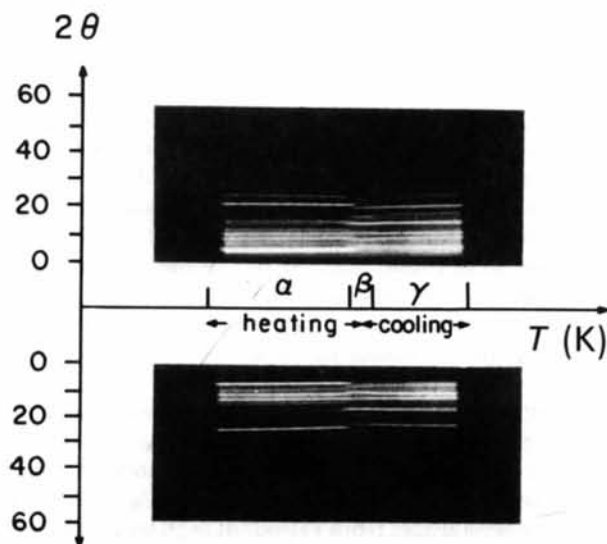


Fig. 3. High-temperature X-ray diffraction photograph of α -TMA with $\text{Cu K}\alpha$ radiation. Specimen heated to 583 K, then gradually cooled to room temperature. Heating/cooling rate was 0.75 K min^{-1} . The photograph shows the following transitions: $\alpha \rightarrow \beta$ (543 K) upon heating and $\beta \rightarrow \gamma$ (553 K) upon cooling.

starting point in the refinement (experimental details in Table 2). Refinement based on the atoms of the three TMA molecules of the asymmetric unit, with isotropic temperature factors, converged at $R = 15.5\%$. Anisotropic refinement of the O atoms of the TMA framework and introduction of the benzene H atoms at calculated positions converged at $R = 11.7\%$. A difference Fourier synthesis computed at this stage showed residual electron densities of about $1 \text{ e } \text{Å}^{-3}$ in the region around $\frac{1}{2}, 0, \frac{1}{2}$. These residual electron densities were interpreted as being due to various decarboxylated species of TMA (*cf.* previous paragraph). These peaks (altogether eight different peaks were identified) were formally assigned as C atoms and added to the refinement. Anisotropic refinement of the non-hydrogen atoms of the TMA framework and isotropic of the ring H atoms (refined as 'riding' atoms) and isotropic refinement of the disordered atoms around $\frac{1}{2}, 0, \frac{1}{2}$ converged to the final agreement factor of $R = 8.4\%$. Block-matrix refinement and unit weights were used during the final cycles of least squares because of the large number of variables (438). A final difference Fourier synthesis showed $\Delta\rho$ excursions in the range -0.41 to $+0.43 \text{ e } \text{Å}^{-3}$ with residual electron densities concentrated in the region around $\frac{1}{2}, 0, \frac{1}{2}$. The largest electron densities in the channel along $0, 0, z$ were $\sim 0.3 \text{ e } \text{Å}^{-3}$. Final atomic parameters of the three TMA molecules (*A*, *B* and *C*) of the asymmetric unit are given in Table 5; coordinates, occupancies and isotropic temperature factors of the disordered atoms around $\frac{1}{2}, 0, \frac{1}{2}$ together with other data have been deposited.

Results and discussion

The TMA framework (made up of 24 TMA molecules per unit cell) has two features of special interest. Thus, the arrangement of molecules *A* and *B* (using the nomenclature employed for TMA.I₅) is such that it leaves channels along the z direction (at $0, 0, z$ and $\frac{1}{2}, \frac{1}{2}, z$). These channels accommodate the polyhalide anion of TMA.I₅. No significant electron densities were found along $0, 0, z$ in the γ -phase and consequently we conclude that the channels are, to a first approximation, empty. The second important feature is the existence of cavities around $\frac{1}{2}, 0, \frac{1}{2}$ and $0, \frac{1}{2}, 0$. These cavities accommodate the water molecules present in TMA.I₅. Significant residual electron densities were found in these regions also in the case of the γ -phase. However, we cannot attribute these peaks to disordered water molecules since the γ -phase crystallizes from vapour at high temperatures and not from solution. We do not believe that there is a contradiction between the occurrence of empty channels and occupied cavities, as the channels allow egress to the exterior while the cavities are totally enclosed within the TMA matrix.

Table 5. Final fractional coordinates of the atoms of the γ -TMA framework ($\times 10^4$), equivalent isotropic temperature factors ($\text{Å}^2 \times 10^3$) for non-hydrogen atoms and isotropic temperature factors for hydrogens ($\text{Å}^2 \times 10^2$)

	<i>x</i>	<i>y</i>	<i>z</i>	$U_{\text{eq}}/U_{\text{iso}}$
C(1)A	1796 (5)	683 (8)	1527 (7)	32 (3)
C(2)A	1554 (5)	894 (9)	2247 (7)	46 (4)
C(3)A	1806 (6)	624 (8)	2966 (8)	44 (4)
C(4)A	2296 (5)	123 (8)	2943 (8)	37 (3)
C(5)A	2523 (4)	-82 (8)	2153 (7)	30 (3)
C(6)A	2276 (5)	193 (9)	1491 (7)	40 (4)
C(7)A	1507 (7)	930 (10)	737 (8)	51 (4)
C(8)A	1560 (5)	908 (9)	3752 (8)	40 (3)
C(9)A	3029 (5)	-607 (8)	2147 (6)	32 (3)
O(1)A	1000 (5)	1097 (9)	768 (6)	86 (4)
O(2)A	1800 (4)	985 (7)	103 (6)	63 (3)
O(3)A	1102 (4)	1247 (9)	3742 (6)	85 (4)
O(4)A	1834 (4)	742 (6)	4384 (5)	43 (3)
O(5)A	3188 (4)	-957 (7)	2819 (6)	65 (3)
O(6)A	3299 (3)	-692 (6)	1520 (5)	42 (2)
C(1)B	588 (5)	1744 (8)	6501 (7)	33 (3)
C(2)B	818 (5)	1472 (8)	7246 (7)	37 (3)
C(3)B	542 (5)	1672 (9)	7938 (7)	41 (4)
C(4)B	52 (5)	2156 (8)	7928 (7)	43 (3)
C(5)B	-158 (4)	2445 (8)	7167 (7)	29 (3)
C(6)B	110 (5)	2243 (8)	6493 (8)	37 (3)
C(7)B	890 (5)	1499 (10)	5766 (8)	46 (4)
C(8)B	780 (6)	1461 (10)	8750 (8)	50 (4)
C(9)B	-664 (5)	3002 (10)	7144 (8)	50 (4)
O(1)B	1324 (4)	1077 (7)	5783 (5)	55 (3)
O(2)B	680 (4)	1781 (8)	5098 (5)	80 (4)
O(3)B	1288 (4)	1225 (8)	8749 (5)	65 (3)
O(4)B	489 (4)	1449 (9)	9369 (6)	81 (4)
O(5)B	-815 (4)	3332 (7)	6510 (5)	59 (3)
O(6)B	-933 (4)	3077 (7)	7788 (6)	75 (3)
C(1)C	8119 (5)	2994 (8)	3690 (7)	37 (3)
C(2)C	7889 (4)	2767 (8)	2940 (7)	36 (3)
C(3)C	8113 (5)	3033 (8)	2209 (7)	38 (3)
C(4)C	8591 (5)	3531 (7)	2226 (8)	43 (3)
C(5)C	8832 (5)	3775 (8)	2974 (7)	36 (3)
C(6)C	8598 (5)	3522 (8)	3676 (7)	38 (3)
C(7)C	7857 (6)	2738 (10)	4462 (7)	49 (4)
C(8)C	7834 (5)	2804 (11)	1438 (7)	52 (5)
C(9)C	9336 (5)	4314 (9)	2990 (7)	39 (3)
O(1)C	7439 (4)	2257 (7)	4441 (5)	67 (3)
O(2)C	8086 (4)	2997 (7)	5086 (5)	67 (3)
O(3)C	7414 (4)	2354 (7)	1461 (5)	63 (3)
O(4)C	8064 (4)	3097 (7)	810 (5)	67 (3)
O(5)C	9549 (4)	4528 (6)	3616 (5)	58 (3)
O(6)C	9544 (4)	4541 (7)	2348 (6)	75 (3)
H(2)A	1175 (5)	1265 (9)	2263 (7)	14 (4)
H(4)A	2493 (5)	-104 (8)	3489 (8)	14 (4)
H(6)A	2454 (5)	42 (9)	909 (7)	14 (4)
H(2)B	1200 (5)	1110 (8)	7265 (7)	10 (3)
H(4)B	-163 (5)	2311 (8)	8481 (7)	10 (3)
H(6)B	-53 (5)	2464 (8)	5921 (8)	10 (3)
H(2)C	7521 (4)	2369 (8)	2930 (7)	5 (2)
H(4)C	8783 (5)	3732 (7)	1667 (8)	5 (2)
H(6)C	8778 (5)	3729 (8)	4240 (7)	5 (2)

There are appreciable and systematic differences between the cell dimensions of γ -TMA and those of TMA.I₅ which we ascribed to small changes in the mode of mutual triple catenation of the TMA networks because of the differences between the species included in the channels and those in the cavity for the two structures. There are significant differences between the final x , y and z coordinates of γ -TMA and those of TMA.I₅. The discrepancies found between the coordinates of molecules *A* and *B* for the two compounds are different from those observed for molecules of type *C*. This different behaviour is to be expected since molecules *A* and *B* participate in the formation of the walls of both the channel and the cavity around $\frac{1}{2}, 0, \frac{1}{2}$, whereas

molecules *C* are involved in the formation of the cavity only. The *x* and *z* coordinates of molecules *A* and *B* in TMA.I₅ and the γ -phase differ by about 10σ ($\sim 0.13 \text{ \AA}$); significantly larger differences (sometimes up to 20σ) were found for the *y* coordinates. The cross section of the channel is rhomboid for both compounds. However, the net result of these changes in the coordinates of molecules *A* and *B* in γ -TMA is the lengthening of the rhombus diagonal along *a* and the shortening of that along *b* (the rhombus angle being 80° in TMA.I₅ and 64° in the γ -phase). The *x* and *y* coordinates of molecules *C* in the two compounds differ by about 10σ , whereas differences as large as 45σ were observed in the case of the *z* coordinates. These differences are most probably due to the fact that the cavities which accommodate water molecules and the proton in TMA.I₅ are filled with TMA or decarboxylated species of TMA in the γ -phase.

Discussion

Interstitial complexes of α -TMA

For smaller guest molecules (Br₂, acetone) the interstitial complexes are formulated as α -TMA. $\frac{1}{6}$ X, with the two molecules in the cavity related by a twofold axis. For larger guest molecules (I₂, hydroquinone, resorcinol) the cavity can contain only one molecule and the formula is α -TMA. $\frac{1}{12}$ X. The guest molecules are strongly held and are only released (as shown by mass spectroscopy) at 523–543 K. We have not investigated whether partial occupation of the cavities occurs if the crystals are grown from more dilute solutions. It is possible that the cavities in α -TMA contain water molecules but this is difficult to establish from density measurements as the composition TMA. $\frac{1}{6}$ H₂O would have a calculated density of 1.47 g cm^{-3} compared to the measured value of 1.46 g cm^{-3} . Unfortunately the region of the cavities was not explored by difference syntheses in the original structure analysis, while the punched-card structure factors are no longer available (Marsh, 1984).

Polymorphism of trimesic acid

Discussion of the structural aspects of the polymorphism of TMA is hindered by the lack of knowledge of the structure of the β -phase not yet obtained as single crystals. Some hydrogen bonds must be broken on melting but the extent to which the hexagonal networks are retained in the melt is not known. However, it does seem clear that enough thermal energy becomes available at $\sim 613 \text{ K}$ to permit breaking of virtually all hydrogen bonds and consequent flash evaporation of the liquid TMA. The γ -phase, grown from the vapour under undefined thermodynamic conditions, retains the mutually

triple-catenated hexagonal TMA networks but in a less closely packed arrangement than the α -TMA. One can define γ -TMA as the hypothetical pure TMA phase with empty channels and cavities. The γ -phase studied here is then a clathrate complex in which the γ -type structure is stabilized by the occupation of the cavities. It is possible that the channels will also be filled with guest molecules if suitable crystallization conditions can be found. We have attempted to obtain such a γ -phase from solutions of TMA and isophthalic acid (see Appendix 2, deposited) but so far without success.

Comparison between the α -TMA and γ -TMA structures

The same hexagonal networks of TMA molecules are found in both structures and these are mutually triply catenated in the same way. The *b* axis in α -TMA and the *c* axis in γ -TMA have virtually the same length because these are the axes parallel to the TMA planes in the two structures. The triple interlacing around the crystallographic twofold axis is similar for both compounds and leads to the formation of cavities of the same kind in the two structures. These accommodate the disordered water molecules of the polyhalide complexes based on the γ -TMA network (see Fig. 8 of Herbstein, Kapon & Reisner, 1981) or disordered TMA and decarboxylated species of TMA in γ -TMA, and the Br₂ molecules of the interstitial complex of α -TMA (see Fig. 1). Here the resemblances end. The planar TMA networks of γ -TMA intersect about the *c* axis to form a channel which is empty in γ -TMA or accommodates polyhalide ions whereas the pleated interlaced networks of α -TMA fill the space efficiently and channels are not formed.

We are grateful to the US–Israel Binational Science Foundation (BSF) and to the Fund for Research at the Technion for financial support of this work. We thank Dr W. Schwotzer (Texas A & M University) who was kind enough to carry out the NMR analysis of TMA. $\frac{1}{12}$ (hydroquinone) and the staff of Israel Mining Industries, Haifa (through the good offices of Dr A. Weissman) for performing the γ -phase NMR spectra. The work on TMA. $\frac{1}{14}$ PA (Appendix 1) was carried out at the California Institute of Technology and we are grateful to Drs R. E. Marsh and S. Samson for their help.

APPENDIX 1

Crystal data for TMA. $\frac{1}{14}$ (picric acid)

When TMA is crystallized from an aqueous solution of picric acid (PA) (TMA:PA ratio in the range 4:1 to 1:1) needles of TMA.H₂O. $\frac{2}{5}$ (PA) (structure by Herbstein & Marsh, 1977) and yellow prisms are

obtained. Chemical analysis shows that the TMA:PA ratio in the prisms is 14:1 (found C 50.07, H 2.73, O 45.75, N 1.32; calculated C 49.95, H 2.77, O 45.91, N 1.33 wt%). The cell dimensions, measured on precession photographs using Co $K\alpha$, are $a = 19.52$ (7), $b = 127.6$ (3), $c = 16.53$ (6) Å. The possible space groups, from systematic absences, are *Ima2* (No. 46) and *Imma* (No. 72). Density was measured by the neutral-buoyancy method in a mixture of CCl_4 and toluene and found to be 1.528 g cm^{-3} ; calculated density is 1.528 g cm^{-3} for 168 TMA + 12PA in the unit cell. The TMA $_{14}$ PA crystals show (70 $\bar{1}$), (701) and (010) faces; no twinning was encountered. The *0kl* reciprocal net shows diffuse bands joining the Bragg reflections in the c^* direction. Dimensional resemblances can be found to both α -TMA and γ -TMA but structural speculations would be premature.

References

- CAHN, R. W. (1954). *Adv. Phys.* **3**, 363-445.
Dictionary of Organic Compounds (1965). 4th ed. London: Eyre and Spottiswoode.

- DUCHAMP, D. J. & MARSH, R. E. (1969). *Acta Cryst.* **B25**, 5-19.
 HERBSTSTEIN, F. H. (1968). *Isr. J. Chem.* **6**, IVp-Vp.
 HERBSTSTEIN, F. H. & KAFTORY, M. (1981). *Z. Kristallogr.* **157**, 1-25.
 HERBSTSTEIN, F. H., KAPON, M. & REISNER, G. M. (1981). *Proc. R. Soc. London Ser. A*, **376**, 301-318.
 HERBSTSTEIN, F. H., KAPON, M. & WEISSMAN, A. (1982). *Isr. J. Chem.* **22**, 207-218.
 HERBSTSTEIN, F. H. & MARSH, R. E. (1977). *Acta Cryst.* **B33**, 2358-2367.
 JOHNSON, C. K. (1965). ORTEP. Report ORNL-3794. Oak Ridge National Laboratory, Tennessee.
 KARLE, I. L. (1955). *J. Chem. Phys.* **23**, 1739.
 KRAUS, M., BERÁNEK, L., KOCHLOEFL, K. & BAŽANT, V. (1962). *Chem. Prum.* **12**, 649-652; *Chem. Abstr.* (1963), **58**, 10746d.
 MARSH, R. E. (1984). Private communication.
 SHELDRICK, G. M. (1977). SHELX77. Program for crystal structure determination. Univ. Cambridge, England.
 SHISHMINA, L. V., BELIKHMAER., YA. A., SARYMSAKOV, SH., KOROLEVA, R. P., SARTOVA, K. A. & ZHUMANALIEVA, N. T. (1982). *Izv. Akad. Nauk Kirg. SSR*, pp. 35-36; *Chem. Abstr.* (1983), **98**, 106912/n.
 SCHOMAKER, V. & MARSH, R. E. (1983). *Acta Cryst.* **A39**, 819-820.
 WEISSMAN, A. (1973). DSc thesis, Technion-Israel Institute of Technology.

Acta Cryst. (1985). **B41**, 354-361

Neutron Diffraction at 15 K and *ab initio* Molecular-Orbital Studies of the Molecular Structure of Carbonohydrazide (Carbohydrazide)

BY G. A. JEFFREY,* J. R. RUBLE,* R. G. NANNI,* A. M. TURANO AND J. H. YATES

Department of Crystallography, University of Pittsburgh, Pittsburgh, PA 15260, USA

(Received 1 December 1984; accepted 13 May 1985)

Abstract

The crystal structure of carbonohydrazide, $(\text{NH}_2\text{NH})_2\text{CO}$, has been refined using single-crystal neutron diffraction data [$\lambda = 1.0470$ (3) Å] measured at 15 K. The crystal data at 15 K are $M_r = 90.1$; $P2_1/c$; $Z = 4$; $a = 3.618$ (1), $b = 8.789$ (3), $c = 12.487$ (5) Å, $\beta = 106.43$ (3)°, $V = 380.9$ (3) Å³; $D_n = 1.571 \text{ Mg m}^{-3}$; $\mu = 257.4 \text{ m}^{-1}$. The final agreement factors are $R(F) = 0.031$, $wR(F^2) = 0.046$, $S = 1.32$ for 1701 observations. The molecule has the *cis/trans/cis/trans* conformation, with significant distortions of the carbon, oxygen and nitrogen atoms from coplanarity. The structures, energies and dipole moments of the eight lowest-energy conformers with approximate C_s symmetry were calculated for the isolated molecules, at rest, by molecular-orbital theory at the HF/3-21G level, using GAUSSIAN80. The lowest-

energy conformer is that observed in the crystal structure. However, the molecular distortions in the crystal correspond to a calculated energy that is 22.8 kJ mol^{-1} above the minimum energy. These distortions arise from a complex system of intra- and intermolecular hydrogen bonds in the crystal.

Introduction

The crystal structure of carbonohydrazide, $(\text{NH}_2\text{NH})_2\text{CO}$, was determined at room temperature by Domiano, Pellinghelli & Tiripicchio (1972). They showed the molecule to have the *cis/trans/cis/trans* conformation shown in (1) in Fig. 1. The structure was re-investigated by Ottersen & Hope (1979) using X-ray data collected at 85 K. This permitted a more precise determination of the hydrogen-atom positions and an electron deformation density analysis. In addition, cell constants of a fully deuterated species have been reported by Baird & Fleming (1974).

The present work was undertaken as part of a series of neutron diffraction molecular structure refinements

* Research Collaborator at Brookhaven National Laboratory, which is operated under contract with the US Department of Energy.